

## Formation of doubly charged molecular ion $\text{Ne}_2^{2+}$ in sub-MeV stripping collision $\text{Ne}_2^+ + \text{Ar} \rightarrow \text{Ne}_2^{2+}$

I. Ben-Itzhak

James R. Macdonald Laboratory, Department of Physics, Kansas State University,  
 Manhattan, Kansas 66506

I. Gertner, D. Bortman, and D. Zajfman\*

Department of Physics, Technion-Israel Institute of Technology, Technion,  
 Haifa 32000, Israel

(Received 1 August 1988; revised manuscript received 22 January 1990)

The first observation of  $\text{Ne}_2^{2+}$  quasimolecular ion obtained by charge stripping of a 900-keV  $\text{Ne}_2^+$  beam in an Ar gas target is reported. This molecular ion has no bound states in the electronic ground state according to previous theoretical calculation.

In this Rapid Communication we report the first observation of the long-lived molecular ion  $\text{Ne}_2^{2+}$ . The  $\text{Ne}_2^{2+}$  was produced by charge stripping of a 900-keV  $\text{Ne}_2^+$  beam in an Ar gas target. A calculation of the adiabatic potential curves of doubly charged molecular ions done by Penkina and Rebane<sup>1</sup> predicted that the  $\text{Ne}_2^{2+}$  molecular ion potential curve has no minimum and is not bound in the ground state.

The apparatus used in the present study has been described in detail previously by Heber *et al.*<sup>2</sup> A schematic diagram of the experimental setup is shown in Fig. 1. A 900-keV  $\text{Ne}_2^+$  beam generated by the Technion 1-MV Van de Graaff accelerator was selected by a  $15^\circ$  analyzing magnet according to their momentum/ $q$ . The beam was collimated to less than  $0.2 \times 0.2 \text{ mm}^2$  at the entrance of the target. A subsequent velocity selector (Wien filter) was used before the target cell to clean the beam from any contamination having a different velocity than  $\text{Ne}_2^+$ . The molecular ions passed through a differentially pumped target cell with 0.3-mm-diam entrance and 3.0-mm exit collimators. The Ar gas pressure in the target cell was typically in the range of  $(0.1-2) \times 10^{-3}$  Torr while the pressure in the rest of the system was kept below  $2 \times 10^{-6}$  Torr.

The doubly charged molecular ion  $\text{Ne}_2^{2+}$ , as well as the  $\text{Ne}^+$  fragments, were deflected by an electrostatic analyzer toward a surface-barrier detector which records a signal proportional to the total energy of each particle detected. Under the same deflector field the  $\text{Ne}_2^+$  beam was directed to a thin gold foil ( $110 \mu\text{g}/\text{cm}^2$ ) and  $\text{Ne}^+$  fragments, scattered from the foil to  $40^\circ$ , were detected by a second detector to monitor the  $\text{Ne}_2^+$  beam current. The use of a gold foil enabled us to measure high incident beam intensities. A typical energy spectrum obtained in the surface-barrier detector is shown in Fig. 2(a). Two energy peaks were always obtained; the higher one, at the full-beam energy, corresponds to events in which either an undissociated molecular ion or both fragments of the dissociated molecular ion arrive simultaneously at the detector; and the lower one, at half-beam energy, corresponds to events in which only one of the fragments arrives at the detector. Thus, the full-energy peak yields the events in the  $2\text{Ne}^+$  and  $\text{Ne}_2^{2+}$  channels. The separation of the counts in the full-energy peak into the  $2\text{Ne}^+$  and  $\text{Ne}_2^{2+}$  channels was done by the grid method described in detail previously.<sup>3-5</sup> The method is based on the different probability for the passage of a single undissociated molecule through a grid as compared with the probability that both

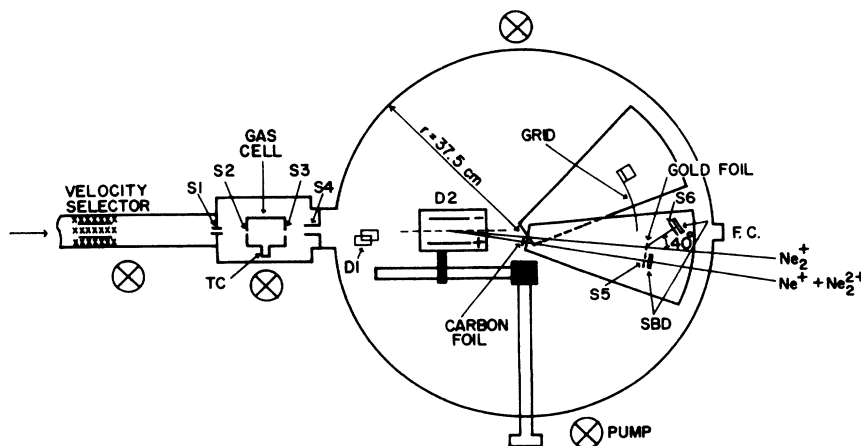


FIG. 1. The experimental setup.

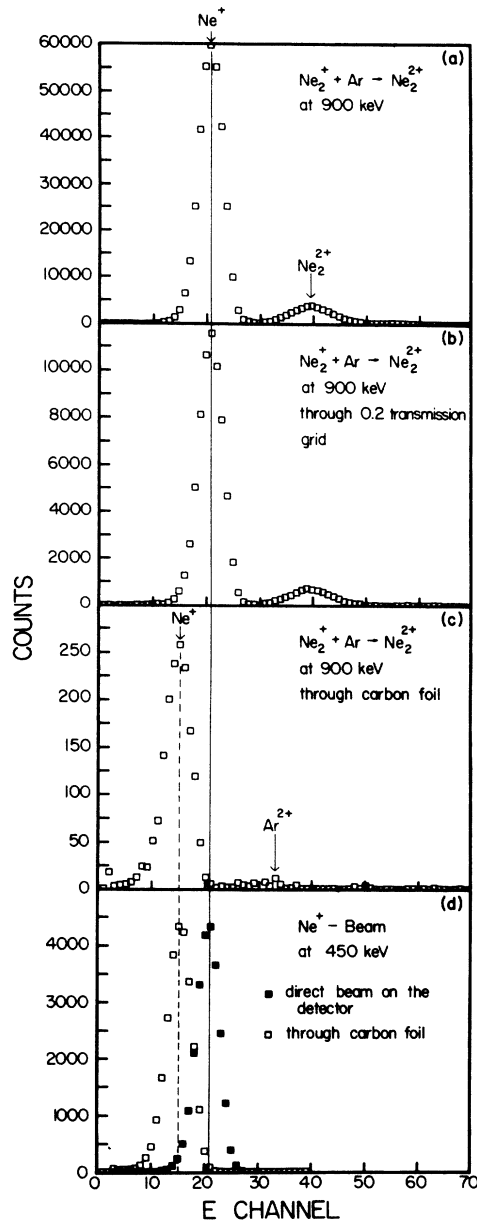


FIG. 2. Energy spectra of (a)  $\text{Ne}^+$  and  $\text{Ne}_2^{2+} + 2\text{Ne}^+$  without the grid, (b)  $\text{Ne}^+$  and  $\text{Ne}_2^{2+} + 2\text{Ne}^+$  with the grid, (c)  $\text{Ne}^+$  and  $\text{Ne}_2^{2+}$  after passing through the carbon foil, and (d) 450-keV  $\text{Ne}^+$  beam directly on the detector and through the carbon foil.

fragments of a dissociated molecule will do the same. Namely, if a fine grid with transmission probability  $T$  is placed in front of a detector, the number of undissociated molecules arriving at the detector will be reduced by the factor  $T$ . On the other hand, the number of two molecular fragments arriving simultaneously to contribute to the full-energy peak will be reduced by the factor  $T^2$  [and there is a probability  $2T(1 - T)$  that one fragment will be stopped in the grid and a probability  $(1 - T)^2$  that both will be stopped by the grid]. This is due to the fact that upon arrival at the grid, the average distance between the two molecular fragments is much larger than the grid con-

stant and they may, therefore, be considered as two independent events in space.

Let  $M$  be the number of counts in a full-energy peak obtained by the detector with no grid, and let  $N$  be the number of counts in the same full-energy peak when a grid with transmission probability  $T$  is placed in front of it (with both measurements normalized to a given number of  $\text{Ne}_2^+$  projectiles); the following relations hold:

$$M = [2\text{Ne}^+] + [\text{Ne}_2^{2+}], \quad (1)$$

$$N = T^2[2\text{Ne}^+] + T[\text{Ne}_2^{2+}], \quad (2)$$

where  $[2\text{Ne}^+]$  and  $[\text{Ne}_2^{2+}]$  are the numbers of  $2\text{Ne}^+$  pairs and  $\text{Ne}_2^{2+}$  molecules, respectively, in this full-energy peak. The relative intensity of the molecular channel is then given by

$$\frac{[\text{Ne}_2^{2+}]}{[2\text{Ne}^+] + [\text{Ne}_2^{2+}]} = (T - T^2)^{-1} \left[ \frac{N}{M} - T^2 \right]. \quad (3)$$

In Fig. 2 we show the energy spectra taken without the grid 2(a) and with the grid 2(b). It can be clearly seen that both the full- and half-energy peaks are reduced approximately by the same factor  $T = 0.2$ , which is the transmission of the grid. Thus, the rate of two  $\text{Ne}^+$  fragments arriving simultaneously is negligible compared to the molecular ions rate. A calculation using Eq. (3) gives

$$\frac{[\text{Ne}_2^{2+}]}{[2\text{Ne}^+] + [\text{Ne}_2^{2+}]} = 0.91. \quad (4)$$

This high ratio of molecular ions to dissociated fragments arriving together is due to the use of the discrimination technique presented by Heber *et al.*<sup>6</sup> A small slit  $0.8 \times 1.1 \text{ mm}^2$  placed on the detector reduces the rate of  $\text{Ne}^+$  fragments without changing the rate of the molecular beam, which is narrower than the slit opening itself. The  $\text{Ne}^+$  fragments have a 2.5-mm-diam spot on the detector due to their kinetic energy in the rest frame of the molecule. The  $\text{Ne}^+$  fragment rate was reduced approximately by

$$s/\pi R^2 \approx 0.18, \quad (5)$$

where  $s$  is the slit opening area and  $R$  is the radius of the fragment spot on the detector.

In order to ascertain that the detected particle was actually the  $\text{Ne}_2^{2+}$  molecular ion and not an  $\text{Ar}^+$  ion, a thin carbon foil was placed on the  $\text{Ne}_2^{2+}$  path after the deflector. This thin carbon foil ( $40 \mu\text{g}/\text{cm}^2$ ) could be put in or out of the doubly charged ions trajectory as shown in Fig. 1, keeping all the experimental conditions the same. Because the foil should dissociate all  $\text{Ne}_2^{2+}$  molecular ions, the energy spectrum is expected to have only a single fragment peak as can be seen in Fig. 2(c). The shift of the peak to lower energy is due to energy loss of the  $\text{Ne}$  fragments in the foil. In Fig. 2(d) we show for comparison the energy spectrum of a 450-keV  $\text{Ne}^+$  beam with and without the carbon foil. The higher peak matches the  $\text{Ne}^+$  fragment peak [Figs. 2(a) and 2(b)], while the lower one matches the  $\text{Ne}$  fragment passing through the carbon foil [Fig. 2(c)]. Since  $\text{Ar}^+$  and  $\text{Ne}_2^+$  follow the same trajectory in the analyzing magnet, there is a possibility of

contamination of the  $\text{Ne}_2^+$  beam. The  $\text{Ar}^+$  can be stripped into  $\text{Ar}^{2+}$  in the target cell and detected as  $\text{Ne}_2^{2+}$  because both of them are detected in the same channel in the energy spectrum. Even a small contamination of  $\text{Ar}^+$  might cause a problem, as the cross section for its stripping is expected to be larger than the one for  $\text{Ne}_2^+$ . From all the methods used only the foil technique enabled us to ascertain that this is not the case. In Fig. 3 we present the energy spectrum of the  $\text{Ne}_2^{2+}$  after passing through the carbon foil. The  $\text{Ar}^{2+}$  peak can be seen in channel 32 as expected due to energy loss in the foil.

For the measurement of the  $\text{Ar}^{2+}$  contamination yield, few modifications of the experimental setup were needed because the multiple scattering of the ions passing through the carbon foil causes broadening of the incident ion beam into a cone having a solid angle much larger than the detection solid angle. First, the carbon foil was changed to a thinner one (about  $7 \mu\text{g}/\text{cm}^2$ ) to minimize the angular broadening. Second, the narrow slit  $S5$  was replaced with an iris aperture, which enabled us to change the detection solid angle. The number of  $\text{Ar}^{2+}$  was measured as a function of the detection solid angle. For each solid angle the measurement was normalized to 50000 counts of  $\text{Ne}^+$  scattered to  $40^\circ$  from the gold foil, and the random  $2\text{Ne}^+$  contribution was subtracted by using the grid method (i.e., two  $\text{Ne}^+$  fragments scattered from the carbon foil into the detector simultaneously). The number of  $\text{Ar}^{2+}$  ions detected as a function of the solid angle are presented in Fig. 4. It can be seen that with an open iris almost all the  $\text{Ar}^{2+}$  ions were detected. The intensity of ions scattered to a given angle  $\theta$  after passing a thin foil is given by<sup>7</sup>

$$F(\theta) = A \exp[-\theta^2 \ln(2)/\theta_{1/2}^2] \quad (6)$$

integrating up to  $\theta_{\text{max}}$  yields,

$$N(\theta_{\text{max}}) = 2\pi A \int_0^{\theta_{\text{max}}} \theta d\theta \exp[-\theta^2 \ln(2)/\theta_{1/2}^2]. \quad (7)$$

The parameter  $\theta_{1/2} = 0.014$  was found by fitting Eq. (7) to the data. The total number of  $\text{Ar}^{2+}$  ions was evaluated to be  $21\,000 \pm 5000$ . The fluctuations in the  $\text{Ar}^{2+}$  yield were

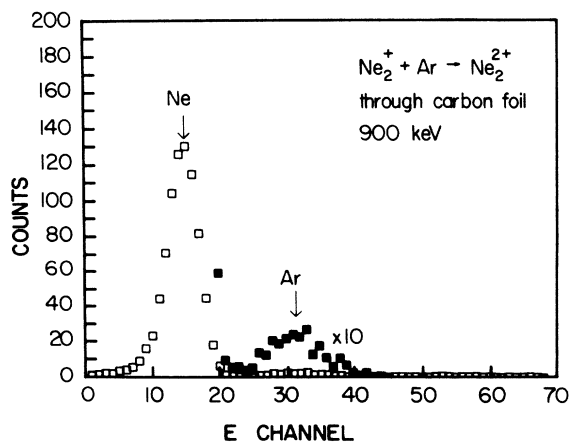


FIG. 3. Energy spectra of  $\text{Ne}_2^{2+}$  after passing through the carbon foil. The  $\text{Ar}^{2+}$  yield was multiplied by a factor of 10.

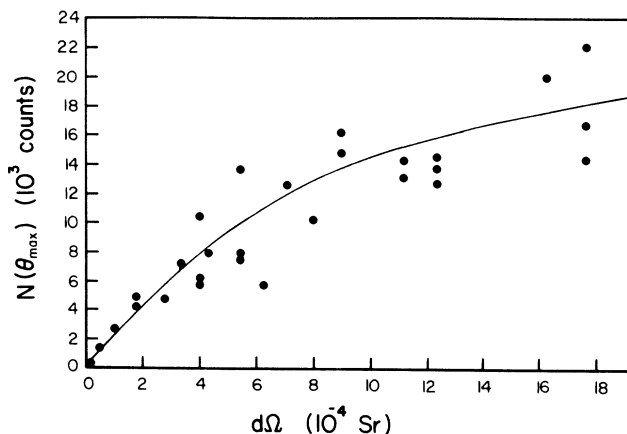


FIG. 4. The number of  $\text{Ar}^{2+}$  ions passing through the thin carbon foil ( $\sim 7 \mu\text{g}/\text{cm}^2$ ) as a function of the detection solid angle, normalized to 50000 counts of  $\text{Ne}^+$  scattered to  $40^\circ$ . The solid line is a fit to multiple scattering theory.

caused mainly by the instability of the  $\text{Ar}^+$  contamination in the beam; similar fluctuations were seen in the yield of  $\text{Ar}^+$  scattered from the gold foil to  $40^\circ$ . Under the same conditions the sum of  $\text{Ne}_2^{2+}$  molecular ions and  $\text{Ar}^{2+}$  ions was  $50\,000 \pm 10\,000$ . Given these numbers the  $\text{Ar}^+$  contamination in the  $\text{Ne}_2^+$  beam can contribute less than 50% of the detected  $\text{Ne}_2^{2+}$ .

A  $\text{CN}_2^+$  molecular ion can be another source of contamination to the  $\text{Ne}_2^+$  beam. This possible contamination is below detection limits as no C or N peaks are detected in the energy spectrum.

In Fig. 5 we present the pressure dependence of the  $\text{Ne}_2^{2+}$  formation normalized to 1000 counts on the normalization detector. The linear dependence at low pressure indicates single-collision conditions. Under these conditions, the beam intensity is approximately independent of the target pressure. The  $\text{Ne}_2^{2+}$  yield at the lowest pressure in the target cell is due to stripping collisions between the velocity selector and the target cell entrance. Using the slope of this curve, the cross section for the stripping process  $\text{Ne}_2^+ + \text{Ar} \rightarrow \text{Ne}_2^{2+}$  was calculated to

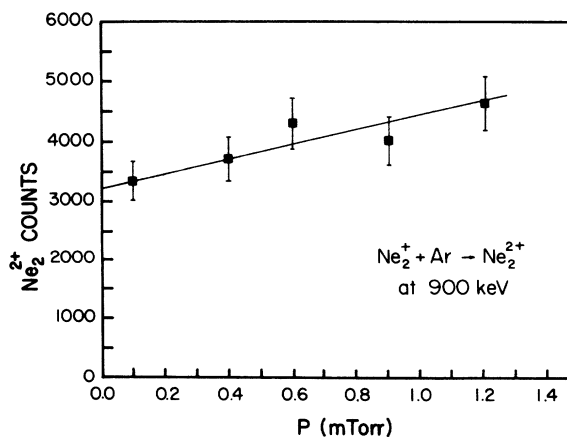


FIG. 5. The yield of  $\text{Ne}_2^{2+}$  as a function of the Ar target pressure.

be of the order of  $10^{-18} \text{ cm}^2$ .

In order to determine the stability of the  $\text{Ne}_2^{2+}$ , the distance between the target cell and the electrostatic deflector was increased. No reduction in the  $\text{Ne}_2^{2+}$  yield within the experimental error was detected. Thus, the  $\text{Ne}_2^{2+}$  has a mean lifetime larger than  $1 \mu\text{sec}$ .

Penkina and Rebane<sup>1</sup> predicted that the  $\text{Ne}_2^{2+}$  is not bound in the electronic ground state since there is no minimum in the adiabatic potential curve. The experimental evidence of its existence suggests that either the detected  $\text{Ne}_2^{2+}$  was in an excited state or that the theoretical approximation used for the  $\text{Ne}_2^{2+}$  ground-state calculation is not accurate enough. A better and more detailed

calculation of doubly charged rare-gas dimers, including the electronically excited state, is needed.

The  $\text{Ne}_2^{2+}$  molecular ion reported here is the fifth observed doubly charged noble gas diatomic molecular ion. The ones reported before are  $\text{NeXe}^{2+}$  by Johnsen and Biondi,<sup>8</sup>  $\text{ArXe}^{2+}$  by Helm *et al.*,<sup>9</sup>  $\text{NeKr}^{2+}$  by Stephan, Mark, and Helm,<sup>10</sup> and  $\text{He}_2^{2+}$  by Guilhaus *et al.*<sup>11</sup>

We thank O. Heber and B. Rosner for many useful discussions. We also thank J. Saban for his invaluable technical assistance. This work was supported in part by the Division of Chemical Sciences, U.S. Department of Energy.

\*Present address: Physics Division, Argonne National Laboratory, Argonne, IL 60439.

<sup>1</sup>N. N. Penkina and T. K. Rebane, *Opt. Spektrosk.* **62**, 514 (1987); **46**, 454 (1979).

<sup>2</sup>O. Heber, I. Gertner, I. Ben-Itzhak, and B. Rosner, *Phys. Rev. A* **38**, 4504 (1988).

<sup>3</sup>T. J. Morgan, K. H. Berkner, and R. V. Pyle, *Phys. Rev. Lett.* **26**, 602 (1971).

<sup>4</sup>J. B. A. Mitchell, J. L. Forand, C. T. Ng, D. P. Levac, R. E. Mitchell, P. M. Mul, W. Claeys, A. Sen, and J. Wm. McGowan, *Phys. Rev. Lett.* **51**, 885 (1983).

<sup>5</sup>S. Abraham, D. Nir, and B. Rosner, *Phys. Rev. A* **29**, 3122

(1984).

<sup>6</sup>O. Heber, I. Ben-Itzhak, I. Gertner, A. Mann, and B. Rosner, *J. Phys. B* **18**, L201 (1985).

<sup>7</sup>L. Meyer, *Phys. Status Solidi (b)* **44**, 253 (1971).

<sup>8</sup>R. Johnsen and M. A. Biondi, *Phys. Rev. A* **20**, 87 (1979).

<sup>9</sup>H. Helm, K. Stephan, T. D. Mark, and D. L. Huestis, *J. Chem. Phys.* **74**, 3844 (1981).

<sup>10</sup>K. Stephan, T. D. Mark, and H. Helm, *Phys. Rev. A* **26**, 2981 (1982).

<sup>11</sup>M. Guilhaus, A. G. Birenton, J. H. Beynon, M. Rabrenovic, and P. Von Raque Schleyer, *J. Phys. B* **17**, L605 (1984).